

# Soft Matter

Accepted Manuscript



This is an *Accepted Manuscript*, which has been through the Royal Society of Chemistry peer review process and has been accepted for publication.

*Accepted Manuscripts* are published online shortly after acceptance, before technical editing, formatting and proof reading. Using this free service, authors can make their results available to the community, in citable form, before we publish the edited article. We will replace this *Accepted Manuscript* with the edited and formatted *Advance Article* as soon as it is available.

You can find more information about *Accepted Manuscripts* in the [Information for Authors](#).

Please note that technical editing may introduce minor changes to the text and/or graphics, which may alter content. The journal's standard [Terms & Conditions](#) and the [Ethical guidelines](#) still apply. In no event shall the Royal Society of Chemistry be held responsible for any errors or omissions in this *Accepted Manuscript* or any consequences arising from the use of any information it contains.

**Self-Assembly of ABC Triblock Copolymer under 3D Soft Confinement: A Monte****Carlo Study**Nan Yan<sup>1,2</sup>, Yutian Zhu<sup>1,\*</sup>, Wei Jiang<sup>1</sup>

*<sup>1</sup>State Key Laboratory of Polymer Physics and Chemistry, Changchun Institute of Applied Chemistry, Chinese Academy of Sciences, Changchun 130022, People's Republic of China*

*<sup>2</sup>University of Chinese Academy of Sciences, Beijing 100049, People's Republic of China*

**Corresponding Author**

\*Tel: +86-43185262866; Fax: +86-43185262126; E-mail [ytzhu@ciac.ac.cn](mailto:ytzhu@ciac.ac.cn)

Under three-dimensional (3D) soft confinement, block copolymers can self-assemble into unique nanostructures that cannot be fabricated in an un-confined space. Linear ABC triblock copolymer containing three chemically distinct polymer blocks possess relatively complex chain architecture, which can be a promising candidate for the 3D confined self-assembly. In the current study, Monte Carlo technique was applied in a lattice model to study the self-assembly of ABC triblock copolymer under 3D soft confinement, which corresponds to the self-assembly of block copolymers confined in emulsion droplets. We demonstrated how to create various nanostructures by tuning the symmetry of ABC triblock copolymers, the incompatibilities between different block types, and solvent properties. Besides common pupa-like and bud-like nanostructures, our simulations predicted various unique self-assembled

nanostructures, including a striped-pattern nanoparticle with intertwined A-cage and C-cage, a pyramid-like nanoparticle with four Janus B-C lamellae adhered onto its four surfaces, a ellipsoidal nanoparticle with a dumbbell-like A-core and two Janus B-C lamellae and a Janus B-C ring surrounded the A-core, a spherical nanoparticle with a A-core and a helical Janus B-C stripe round the A-core, a cubic nanoparticle with a cube-shape A-core and six Janus B-C lamellae adhered onto the surfaces of A-cube, and a spherical nanoparticle with helical A, B and C structures, from the 3D confined self-assembly of ABC triblock copolymers. Moreover, the formation mechanisms of some typical nanostructures were also examined by the variations of the contact numbers with time and a series of snapshots at different Monte Carlo time. It is found that ABC triblock copolymers usually aggregate into a loose aggregate at first, and then the microphase separation between A, B and C blocks occurs, resulting in the formation of various nanostructures.

## Introduction

Recently, the self-assembly of block copolymers (BCPs) under 3D confinement has attracted increasing attention since the confinement effect can effectively break the symmetry of a structure, resulting in some new nanostructures that cannot be obtained by other methods.<sup>1-8</sup> Up to now, great efforts have been made to fabricate block copolymer nanoparticles with abundant internal microphase-separated nanostructures due to their potential applications as catalyst carrier, dielectric resonators, drug delivery system, and photonic crystals.<sup>9, 10</sup> Basically, the confinements can be divided

into two categories, hard confinement and soft confinement.<sup>7</sup> If the confining boundary is the hard surface, the shape of the confining geometry is always fixed. This kind of confinement is termed hard confinement. In contrast to hard confinement, soft confinement refers to the confinement when the confining geometry is not fixed but deformable, such as the cells or emulsion droplets.

When confined within a spherical space, BCPs can spontaneously self-assemble into a variety of unique nanostructures, depending on various control parameters, including the size of the confined space, the intrinsic property of BCP, polymer-surface interactions, and so forth.<sup>1, 11-19</sup> For instance, Liang and coworkers investigated the self-assembly of AB diblock copolymers confined in a solid spherical space via Monte Carlo method.<sup>1</sup> It was found that the symmetric diblock copolymers are more likely to form the onion-like multilayer structure. Yu et al. predicted a large number of interesting patchy nanoparticles self-assembled from linear triblock copolymers under solid spherical confinement.<sup>19</sup> Compare to the self-assembly under solid confinement, the self-assembly of block copolymer confined in the emulsion droplet, i.e. under 3D soft confinement, has received more and more attention these years. For example, Zhu and coworkers fabricated mesoporous BCP nanoparticles with tailored pore structures, taking advantage of supramolecular chemistry and 3D confined assembly of block copolymers.<sup>14</sup> Yang and Zhu generated nanostructured particles via the self-assembly of polystyrene-*b*-poly (4-vinylpyridine) (pentadecyphenol) (PS-*b*-P4VP (PDP)) under 3D soft confinement.<sup>15</sup> The internal structures of the resulting nanoparticles can be readily tuned by varying PDP content.

Yi and Yang obtained various unprecedented structural motifs by cooperative self-assembly of block copolymers and amphiphilic block copolymer surfactant within emulsion droplets.<sup>13</sup> Besides experimental works, Li and coworkers recently proposed a simulated annealing method to mimic the self-assembly of diblock copolymers confined in the emulsion droplets.<sup>7</sup> The soft confinement was achieved by the formation of polymer droplets in a poor solvent environment, which corresponded well with the self-assembly of block copolymer confined in emulsion droplets.

On the other hand, it has been reported that linear ABC triblock copolymer, comprised of three chemically distinct polymer blocks covalently linked together, is a versatile precursor for the fabrication of various interesting multicompartment micelles, such as helices, raspberry-like particles, hamburger-like particles, Janus particles, segmented cylinders, and segmented wormlike micelles.<sup>20-32</sup> For example, Zhu *et al.* fabricated the giant segmented wormlike micelles from the self-assembly of linear poly(styrene-*b*-2-vinylpyridine-*b*-ethylene oxide) triblock copolymer in a dilute solution.<sup>16</sup> Liu and coworkers reported the unique double helices from the self-assembly of poly(*n*-butyl methacrylate)-*b*-poly(2-cinnamoyloxyethyl methacrylate)-*b*-poly(*tert*-butyl acrylate) (PBMA-*b*-PCEMA-*b*-PtBA) triblock copolymer.<sup>24</sup> However, self-assembly of ABC triblock copolymer under 3D soft confinement was seldom investigated whether in experiments or in computer simulations. Very recently, Zhu and coworkers examined the self-assembly of polystyrene-*b*-polyisoprene-*b*-poly(2-vinylpyridine) confined in emulsion droplets.<sup>17</sup> They observed the morphologies of the self-assembled nanoparticles can be tuned

from onion-like to bud-like, pupa-like, and then to reversed pupa-like and onion-like particles by tailoring the properties of the surfactants. Because of the complex chain architecture of ABC triblock copolymer and the relatively complicated interactions among the three blocks and the interface, it is far away from a clear understanding of the self-assembly of ABC triblock copolymer under the 3D soft confinement.

In the current study, we applied Monte Carlo simulation to systematically investigate the self-assembly of linear ABC triblock copolymers under 3D soft confinement. The simulations predicted a rich variety of unique self-assembled nanostructures from the self-assembly of ABC triblock copolymer under 3D soft confinement. Moreover, the formation mechanisms for some typical nanoparticles were also examined.

### **Model and method**

Monte Carlo method was performed in this work to mimic the self-assembly of linear ABC triblock copolymers under 3D soft confinement. All the simulations were carried out in a  $50 \times 50 \times 50$  simple cubic lattice by the self-avoiding chain model. Periodic boundary condition was imposed in all three directions. The single-site bond fluctuation model with restricting the bond length either 1 or  $\sqrt{2}$  was used.<sup>33-35</sup> Excluded volume interactions were always enforced to ensure that no more than one monomer occupied the same lattice site and no bond crossing was allowed. This means each lattice site is occupied by either a polymer bead or a vacancy (a solvent). Evolution of the polymer chain was achieved through the exchange move between the

polymer bead and vacancy. A polymer bead was chosen randomly to make an attempted exchange with one of its 18 nearest-neighbor sites. To enhance the simulation efficiency, the partial-reptation algorithm was applied only if the selected polymer bead cannot make an exchange with any of the 18 nearest-neighbor sites because of the violation of excluded volume conditions or the no bond-crossing or the bond length restrictions.<sup>36, 37</sup> The acceptance or rejection of the attempted exchange was further determined by the Metropolis rule.<sup>38</sup> This rule states that the attempted exchange is accepted if the energy change  $\Delta E$  is negative. Otherwise, the exchange will be accepted with a probability of  $p = \exp[-\Delta E / k_B T]$ , where  $\Delta E = \sum_{ij} \Delta N_{ij} \varepsilon_{ij}$  is the energy change in one attempted exchange;  $k_B$  is the Boltzmann constant and set as 1;  $T$  is the reduced temperature,  $\Delta N_{ij}$  is the number difference between the nearest neighbor pairs of components  $i$  and  $j$  before and after the exchange,  $\varepsilon_{ij}$  is the reduced interaction between components  $i$  and  $j$ ;  $i, j = A, B, C$  and  $S$  (solvent), respectively.

In experiments of the emulsion-evaporation induced self-assembly, BCPs were dissolved in organic solvent (good solvent) at first, and then were emulsified in water (poor solvent). As the organic solvent was evaporated, BCPs tended to aggregate into a polymer droplet, which was surrounded by the water. On the hand, the microphase separation between the different block types occurred simultaneity, resulting in a large number of well defined nanostructures. In the previous works, the annealing method was proposed to mimic the emulsion-evaporation induced self-assembly in experiments.<sup>7, 18</sup> In simulations, the inverse temperature  $1/T$  changed gradually

from 0 (an athermal state of  $T=\infty$ ) to 0.07, which represents the system changing from an athermal state to a relatively low temperature state. The annealing rate was kept at 0.0002 per step in this study. This annealing process caused BCPs gradually aggregating into the polymer droplets when solvent environment is changed from a good solvent to a poor solvent, corresponding well to emulsion-evaporation induced self-assembly of polymer in experiments. The annealing process was completed in 350 steps at an annealing rate of 0.0002 per step. After the annealing process,  $1/T$  was kept as 0.07, and another 650 annealing steps were carried out to ensure that the final structures were under an equilibrium state. In each annealing step, 9000 Monte Carlo steps (MCSs) were performed. One MCS means each bead has one attempted exchange move on average.

In all the simulations, the concentration of the block copolymers was fixed as 10 % (i.e. 595 polymer chains in the system) and the chain length was set as  $Le = 21$ , i.e.  $L_A + L_B + L_C = 21$ . All other self-interactions between the same components, i.e.  $\epsilon_{AA}$ ,  $\epsilon_{BB}$ ,  $\epsilon_{CC}$ , and  $\epsilon_{SS}$  were set as 0. The polymer-polymer interactions between the different polymer components were set as  $\epsilon_{AB} = \epsilon_{AC} = \epsilon_{BC} = 3.0$  to mimic the incompatibilities between different block types. The polymer-solvent interactions,  $\epsilon_{AS}$ ,  $\epsilon_{BS}$  and  $\epsilon_{CS}$ , were set to positive values to ensure the solvent is poor for all the blocks.

## Results and discussion

Clearly, the confined self-assembly of ABC triblock copolymer is largely dominated by a series of controlling parameters, including polymer-polymer



interactions, polymer-solvent interactions and the length ratios of A, B and C blocks. The influence of these parameters on the self-assembled nanostructure is considered in this study. Figure 1 shows a series of aggregates from the symmetrical  $A_7B_7C_7$  triblock copolymers at different polymer-solvent interactions. When  $\epsilon_{AS} < \epsilon_{BS} < \epsilon_{CS}$  ( $\epsilon_{AS} = 1.0$ ,  $\epsilon_{BS} = 2.0$  and  $\epsilon_{CS} = 3.0$ , Figure 1a),  $A_7B_7C_7$  triblock copolymers aggregate into a tapered nanoparticle with the weak hydrophobic A lamellae covered at bottom and top of the nanoparticle. This tapered nanoparticle is similar to the bud-like nanoparticle in experiments.<sup>17</sup> When A, B, and C blocks possess the same hydrophobicity (i.e.  $\epsilon_{AS} = \epsilon_{BS} = \epsilon_{CS} = 3.0$ ), an ellipsoidal pupa-like nanoparticle is formed by  $A_7B_7C_7$  triblock copolymers, as shown in Figure 1b. When the hydrophobicity of A, B and C blocks are decreases progressively, a reversed bud-like nanoparticle is observed, as shown in Figure 1c. This morphological transition from bud-like particle to pupa-like particle, and then to reversed bud-like particle agrees well with the experimental observation.<sup>17</sup> The simulation results indicate that the terminal blocks (A or C block) with weaker hydrophobicity are always at the bottom and top of the bud-like particle to reduce the energy of system.<sup>39</sup>

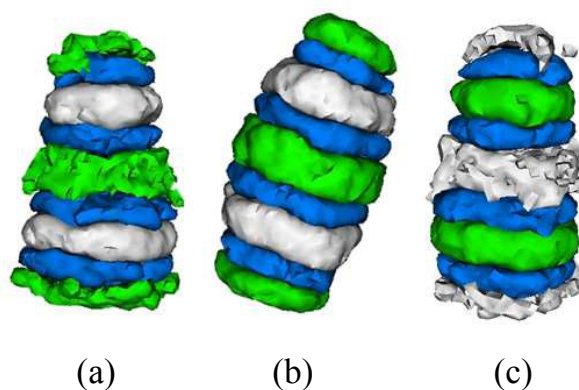


**Figure 1.** Typical aggregates from symmetrical  $A_7B_7C_7$  triblock copolymer at different  $\epsilon_{AS}$ ,  $\epsilon_{BS}$ ,

and  $\epsilon_{CS}$ . (a)  $\epsilon_{AS}=1.0$ ,  $\epsilon_{BS}=2.0$  and  $\epsilon_{CS}=3.0$ ; (b)  $\epsilon_{AS}=\epsilon_{BS}=\epsilon_{CS}=3.0$ ; (c)  $\epsilon_{AS}=3.0$ ,  $\epsilon_{BS}=2.0$  and  $\epsilon_{CS}=1.0$ .  $\epsilon_{AB}=\epsilon_{BC}=\epsilon_{AC}=3.0$  for (a-c).  $\square$  represents the A blocks;  $\square$  represents the B blocks;  $\square$  represents the C blocks.

Comparing to the symmetrical block copolymers, more unique nanostructures may be obtained from the self-assembly of asymmetrical block copolymers due to their asymmetric chain architectures. In the current study, three types of asymmetrical ABC triblock copolymers, i.e.  $A_4B_{13}C_4$ ,  $A_{13}B_4C_4$  and  $A_8B_5C_8$  are considered in the following section. In these asymmetric block copolymers,  $A_4B_{13}C_4$  possesses a relatively long middle block,  $A_{13}B_4C_4$  contains a relatively long terminal block, whereas  $A_8B_5C_8$  has two long terminal blocks and a short middle block. Figure 2 shows a series of typical aggregates formed by  $A_4B_{13}C_4$  triblock copolymers as a function of polymer-solvent interaction (i.e.  $\epsilon_{PS}$ , we set  $\epsilon_{PS}=\epsilon_{AS}=\epsilon_{BS}=\epsilon_{CS}$ ). When  $\epsilon_{PS} \leq 5.0$ , ABC triblock copolymers tend to aggregate into a novel nanostructure with a striped-pattern on the surface of the nanoparticle. From the top images, it is observed that A and C blocks tend to form the cage-like structure. More interestingly, A-cage and C-cage are intertwined with each other, as shown in Figure 2. As  $\epsilon_{PS}$  is increased, A and C stripes start to break up into some short stripes ( $\epsilon_{PS}=6.0$ ), and then into a larger number of small patches ( $\epsilon_{PS}=8.0$  or  $\epsilon_{PS}=10.0$ ). As the increase of the hydrophobicity,  $A_4B_{13}C_4$  triblock copolymers tend to aggregate into a more compact nanoparticle to reduce the contact between the hydrophobic blocks and the solvents. Because of the shrink of nanoparticle, the short A and C blocks can no longer form long stripes, which can only form some small patches embedded in the porous B shell.

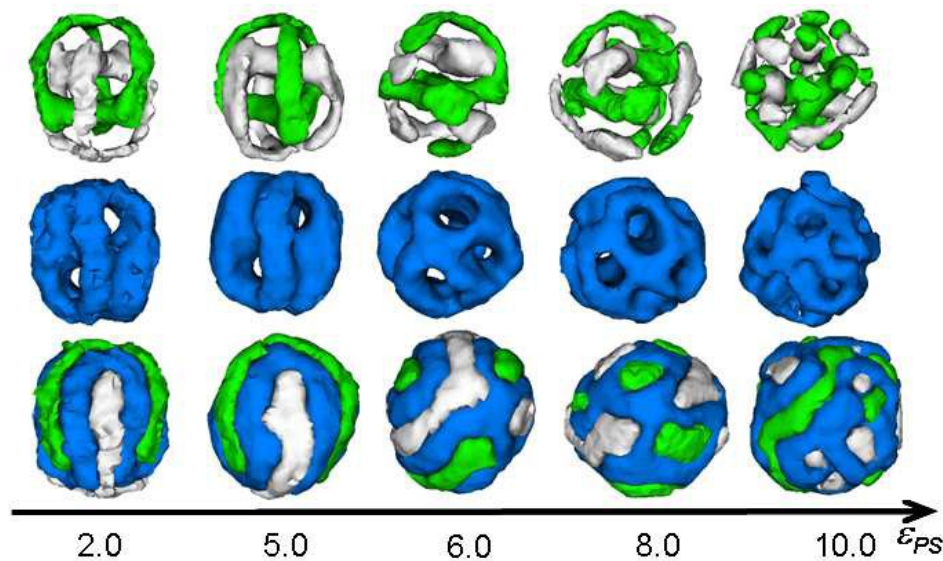


**Figure 2.** A series of typical aggregates from asymmetrical  $A_4B_{13}C_4$  triblock copolymer as a function of  $\epsilon_{PS}$ .  $\epsilon_{PS}=\epsilon_{AS}=\epsilon_{BS}=\epsilon_{CS}$  and  $\epsilon_{AB}=\epsilon_{BC}=\epsilon_{AC}=3.0$ . The color codes are the same as that in Figure 1.

In Figure 2, A, B and C blocks possess the same hydrophobicity, i.e.  $\epsilon_{AS}=\epsilon_{BS}=\epsilon_{CS}$ . Clearly, the hydrophobicity of each block also plays an important role in the self-assembly. The blocks with weaker hydrophobicity are more likely to distribute on the surface of the aggregated nanoparticle, whereas the blocks with stronger hydrophobicity tend to form the inner core to avoid the contact with the solvents. To examine the effect of hydrophobicity of each block on the self-assembled nanostructures, we present a series of aggregated morphologies of  $A_4B_{13}C_4$  triblock copolymers with different  $\epsilon_{AS}$ ,  $\epsilon_{BS}$  and  $\epsilon_{CS}$  in Figure 3. When A blocks possess relatively higher hydrophobicity than the B and C blocks (i.e.  $\epsilon_{AS}=4.0$  and  $\epsilon_{BS}=\epsilon_{CS}=2.0$ , Figure 3a), A blocks tend to aggregate into a polygonal core, whereas B and C blocks form a porous shell and cage, respectively. On the contrary, C blocks are more likely

to aggregate into a pentacle core, and B and A blocks form the porous shell and cage respectively, when B and C blocks are more hydrophobic than the A blocks ( $\epsilon_{AS}=2.0$  and  $\epsilon_{BS}=\epsilon_{CS}=4.0$ , Figure 3b). When the middle B blocks are more hydrophobic than the two terminal blocks, i.e. A and C blocks, ABC triblock copolymers self-assemble into a nanoparticles with A and C stripes on the surface ( $\epsilon_{AS}=\epsilon_{CS}=2.0$  and  $\epsilon_{BS}=5.0$ , Figure 3c). It is interesting to observe that A and C blocks form two hemispheres in the center of the nanoparticle, as shown in the top images of Figure 3c. When the A and C blocks possess higher hydrophobicity than the middle B blocks ( $\epsilon_{AS}=\epsilon_{CS}=5.0$  and  $\epsilon_{BS}=2.0$ ), ABC triblock copolymers form a patch-like nanoparticle, as shown in Figure 3d. This patch-like nanoparticle is composed of a large number of small A and C spheres and a porous B shell.

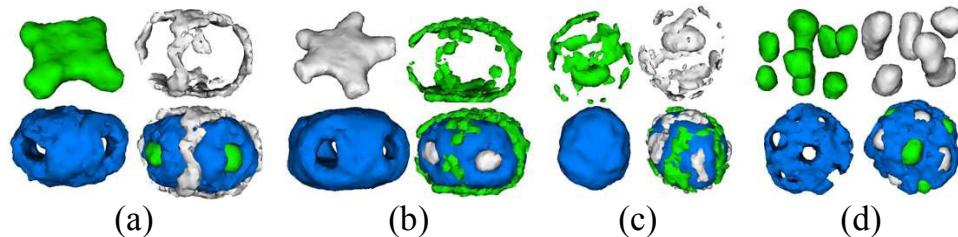


**Figure 3.** Typical aggregates from asymmetrical  $A_4B_{13}C_4$  triblock copolymer at different  $\epsilon_{AS}$ ,  $\epsilon_{BS}$  and  $\epsilon_{CS}$ . (a)  $\epsilon_{AS}=4.0$ ,  $\epsilon_{BS}=\epsilon_{CS}=2.0$ ; (b)  $\epsilon_{AS}=2.0$ ,  $\epsilon_{BS}=\epsilon_{CS}=4.0$ ; (c)  $\epsilon_{AS}=\epsilon_{CS}=2.0$ ,  $\epsilon_{BS}=5.0$ ; (d)  $\epsilon_{AS}=\epsilon_{CS}=5.0$ ,  $\epsilon_{BS}=2.0$ . The color codes are the same as that in Figure 1.

The confined self-assembly of asymmetrical  $A_{13}B_4C_4$  triblock copolymer is also examined. Figure 4 presents the typical aggregates formed by  $A_{13}B_4C_4$  triblock copolymers as a function of  $\epsilon_{PS}$  ( $\epsilon_{PS}=\epsilon_{AS}=\epsilon_{BS}=\epsilon_{CS}$ ). When  $\epsilon_{PS}=2.0$ ,  $A_{13}B_4C_4$  triblock copolymers aggregate into a pyramid-like nanoparticle, as shown in Figure 4. It is interesting to note that B and C blocks form four Janus lamellae adhered onto the four

surfaces of the pyramid-like nanoparticle. As  $\epsilon_{PS}$  is increased to 3.0, A blocks are more likely to form a dumbbell-like core, while B and C assemble into two Janus lamellae and a Janus ring surrounded the A-core. As  $\epsilon_{PS}$  is further increased, isolated Janus B-C lamellae tend to coalesce into one Janus stripe, as shown in images in Figure 4 ( $\epsilon_{PS}=6.0$  and  $\epsilon_{PS}=8.0$ ). More interesting, B and C form a helical Janus stripe round the A-core when  $\epsilon_{PS}$  is 8.0. As the hydrophobic degree is increased from 2.0 to 8.0, the shape of the self-assembled nanoparticle transitions from tetrahedron ( $\epsilon_{PS}=2.0$ ) to ellipsoid ( $\epsilon_{PS}=3.0$ ), and then to sphere ( $\epsilon_{PS}=6.0$  and  $\epsilon_{PS}=8.0$ ). Clearly, this transition can effectively reduce the surface area of the nanoparticle, which can decrease the contacts between the hydrophobic blocks and the poor solvents.

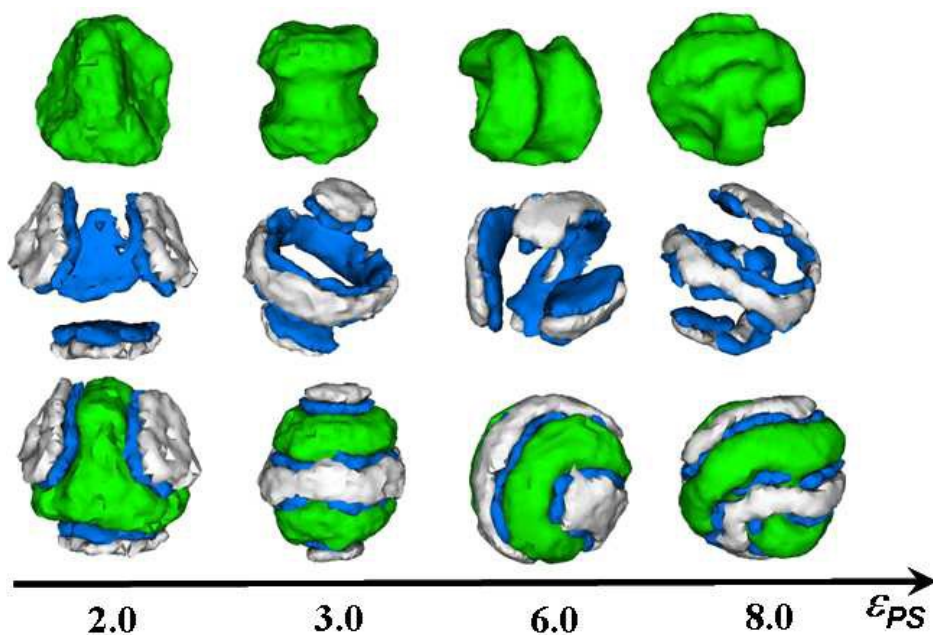


**Figure 4.** A series of typical aggregates from asymmetrical  $A_{13}B_4C_4$  triblock copolymer as a function of  $\epsilon_{PS}$ .  $\epsilon_{PS}=\epsilon_{AS}=\epsilon_{BS}=\epsilon_{CS}$  and  $\epsilon_{AB}=\epsilon_{BC}=\epsilon_{AC}=3.0$ . The color codes are the same as that in Figure 1.

In Figure 5, we present a series of typical aggregates from asymmetrical  $A_{13}B_4C_4$

triblock copolymer when A, B and C blocks possess different hydrophobic properties. When the hydrophobic properties of A, B and C blocks are decreased in turn ( $\epsilon_{AS}=4.0$ ,  $\epsilon_{BS}=3.0$ ,  $\epsilon_{CS}=2.0$ ), ABC triblock copolymers aggregate into a novel cubic nanoparticle (Figure 5a). It can be seen that the highly hydrophobic A blocks form a cube-shape core, whereas the weak hydrophobic B and C blocks form six Janus lamellae adhered onto the surfaces of A-cube. Moreover, it is observed parts of B and C blocks co-assemble into an inner core embedded inside the A-cube. When C blocks possess higher hydrophobicity than those of A and B blocks ( $\epsilon_{AS}=\epsilon_{BS}=2.0$ ,  $\epsilon_{CS}=4.0$ ), A blocks form a W-shape shell, whereas B and C blocks form the curved lamellae and short rods respectively filled in the cracks of the W-shape A shell (Figure 5b). In this nanostructure, the highly hydrophobic C blocks are embedded, which can minimize their exposures in poor solvent environment. When the middle B block has higher hydrophobicity than the A and C blocks ( $\epsilon_{AS}=\epsilon_{CS}=2.0$ ,  $\epsilon_{BS}=6.0$ ), A block form a dumbbell-shape core, B and C form the Janus lamellae and ring surrounded the dumbbell-shape A-core (Figure 5c), which is similar to the self-assembled nanostructure shown in Figure 4 (images at  $\epsilon_{AS}=\epsilon_{BS}=\epsilon_{CS}=3.0$ ).



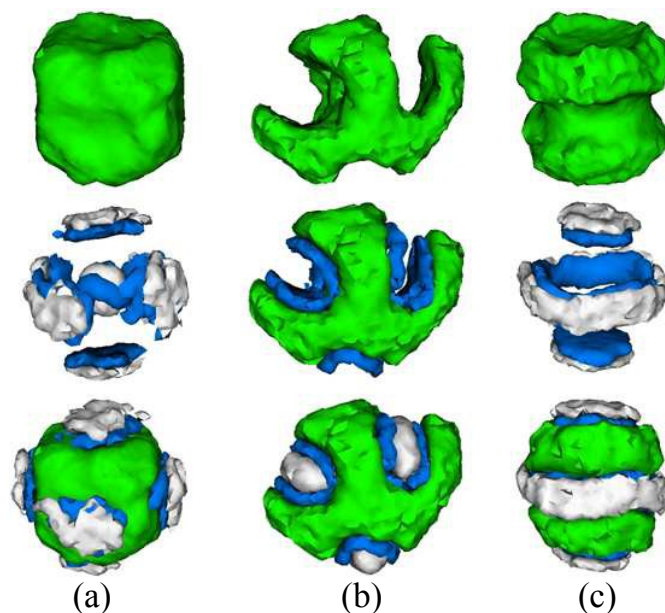


**Figure 5.** Typical aggregates from asymmetrical  $A_{13}B_4C_4$  triblock copolymer at different  $\epsilon_{AS}$ ,  $\epsilon_{BS}$  and  $\epsilon_{CS}$ . (a)  $\epsilon_{AS}=4.0$ ,  $\epsilon_{BS}=3.0$ ,  $\epsilon_{CS}=2.0$ ; (b)  $\epsilon_{AS}=\epsilon_{BS}=2.0$ ,  $\epsilon_{CS}=4.0$ ; (c)  $\epsilon_{AS}=\epsilon_{CS}=2.0$ ,  $\epsilon_{BS}=6.0$ . The color codes are the same as that in Figure 1.

For the asymmetrical  $A_8B_5C_8$  triblock copolymer, it contains two relatively long end blocks (A and C blocks) and a relatively short middle B block, which has different chain architecture from the asymmetrical  $A_4B_{13}C_4$  and  $A_{13}B_4C_4$  copolymers. A series of resulting aggregates at different polymer-solvent interaction ( $\epsilon_{PS}$ ) are presented in Figure 6. When  $\epsilon_{PS}=3.0$  or  $\epsilon_{PS}=6.0$ , a classic pupa-like particle containing the A-B-C alternating structure is observed. As  $\epsilon_{PS}$  is increased ( $\epsilon_{PS}=7.0$  or  $\epsilon_{PS}=8.0$ ), parallel A, B and C lamellae transition into the distorted lamellae. Moreover, it is interesting to note that A, B and C are more likely to form the helical structures when  $\epsilon_{PS}$  is increased to 9.0, as shown in Figure 6. From the images at  $\epsilon_{PS}=9.0$ , it is observed that the two end blocks, i.e. A and C blocks, form the helical structures, whereas the middle B blocks aggregate into a double-helix structure.

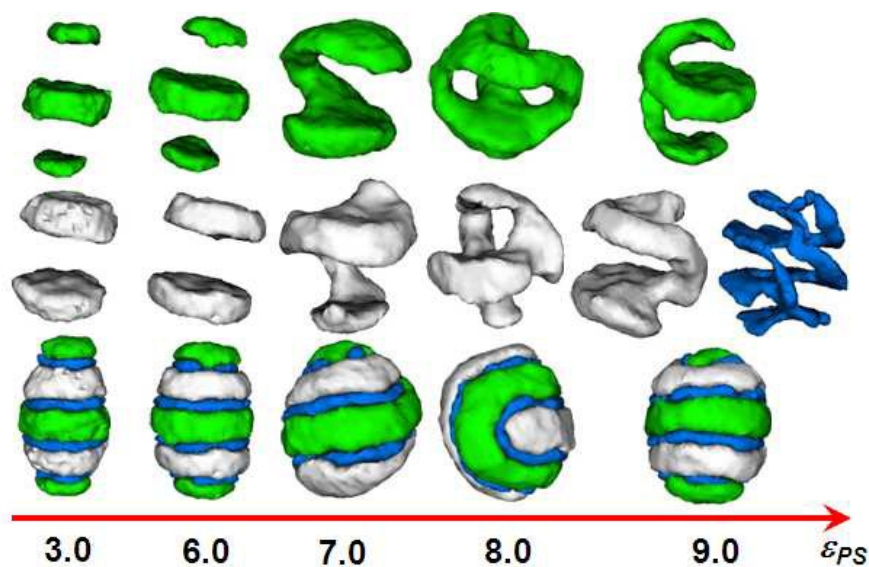
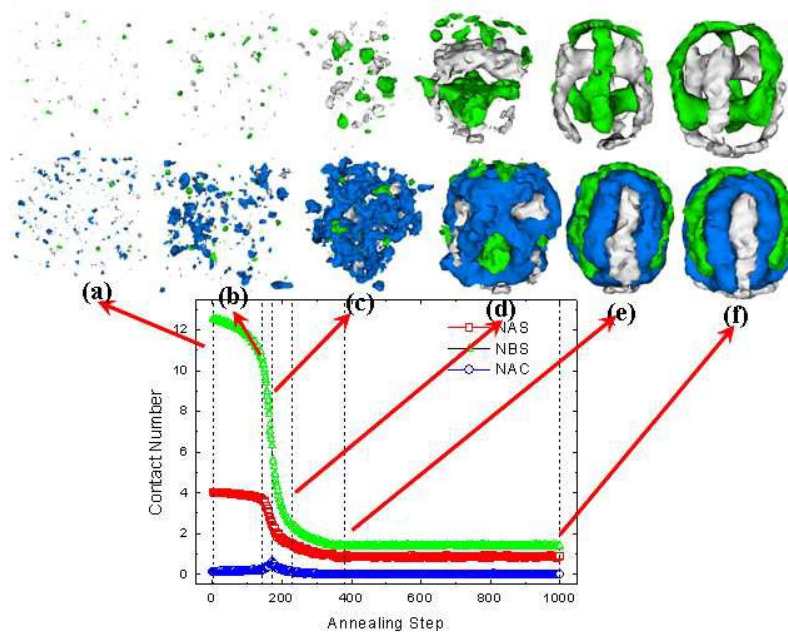


**Figure 6.** A series of typical aggregates from asymmetrical  $A_8B_5C_8$  triblock copolymer as a function of  $\epsilon_{PS}$ .  $\epsilon_{PS}=\epsilon_{AS}=\epsilon_{BS}=\epsilon_{CS}$  and  $\epsilon_{AB}=\epsilon_{BC}=\epsilon_{AC}=3.0$ . The color codes are the same as that in Figure 1.

Until now, very limited information is available for the formation pathway of the micelles because the difficult in tracing the morphological transition by the off-line technique such as transmission electron microscopy (TEM). Monte Carlo simulation has been proved to be an effective method to explore the kinematic pathway for the self-assembled micelles.<sup>18, 28, 40-42</sup> In the following section, the formation mechanisms of some novel self-assembled nanoparticles are examined. Figure 7 presents the variations of the contact numbers ( $N_{AS}$ ,  $N_{BS}$  and  $N_{AC}$ ) with time for the  $A_4B_{13}C_4$  triblock copolymer at  $\epsilon_{AS}=\epsilon_{BS}=\epsilon_{CS}=2.0$ . At this interaction setting,  $A_4B_{13}C_4$  triblock copolymers aggregate into a striped-pattern nanoparticle with intertwined A-cage and C-cage, as shown in Figure 2. To visualize the formation pathway of this novel nanostructure, a series of snapshots at different times are also inserted in Figure 7.  $N_{AS}$  and  $N_{BS}$  are the contact numbers between monomers (A or B) and solvents, indicating



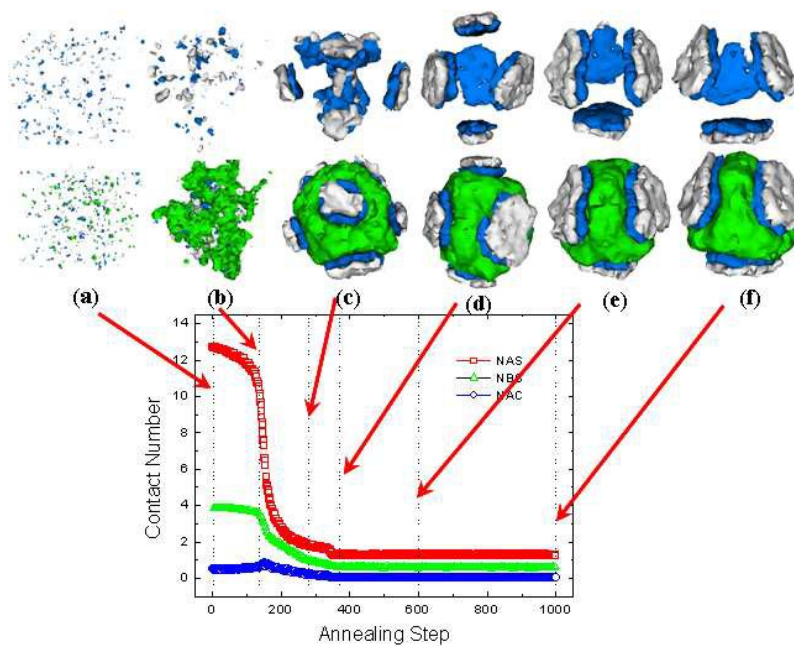
the micellization of block copolymer.  $N_{AC}$  is the contact number between the immiscible A and C monomers, which can be used to monitor the microphase separation between the A and C blocks. As can be seen from the  $N_{AS}-t$  and  $N_{BS}-t$  curves,  $N_{AS}$  and  $N_{BS}$  show a steady decline with time until  $t=380$  (micellization), and then remain mostly unchanged as time further increases (micellization completed).  $N_{AC}$  increases considerably with time and then reaches its peak at  $t=170$ . Thereafter,  $N_{AC}$  slightly decreases with time till  $t=380$ , and then remains unchanged as time further increases. Clearly, the contact between A and C will increase when the randomly dispersed ABC triblock copolymers aggregate into a polymer droplet under soft confinement. Therefore, the initial  $N_{AC}$  increase of with time is attributed to the aggregation of  $A_4B_{13}C_4$  triblock copolymers, whereas the subsequent decrease of  $N_{AC}$  is caused by the microphase separation between the immiscible A and C blocks. The formation pathway of the resulting striped-pattern is visualized by a series inserted snapshots of the block copolymers. It is observed that the  $A_4B_{13}C_4$  triblock copolymers gradually aggregate together (Figure 7a and 7b) at first, and then form a loose aggregate at  $t=170$  (Figure 7c), when the quality of solvent gradually transitions from good solvent to poor solvent. Thereafter, the microphase separation between A, B and C occurs, resulting in the formation of a more compact nanoparticle with the striped-pattern (Figure 7d and 7e,  $380 \leq t \leq 230$ ). In striped-pattern nanoparticle, A and C blocks form two cages intertwined with each other. This striped-pattern structure remains almost unchanged as the annealing step further increases (Figure 7f,  $t=1000$ ).



**Figure 7.** Variations of the numbers of contacts,  $N_{AS}$ ,  $N_{BS}$  and  $N_{AC}$ , with time for asymmetrical  $A_4B_{13}C_4$  triblock copolymer at  $\varepsilon_{AS}=\varepsilon_{BS}=\varepsilon_{CS}=2.0$ . Typical snapshots at different times are also inserted in this diagram to show the formation pathway of the striped-pattern nanoparticle with intertwined A-cage and C-cage: (a)  $t=1$ ; (b)  $t=141$ ; (c)  $t=170$ ; (d)  $t=230$ ; (e)  $t=380$ ; (f)  $t=1000$ . The color codes for the snapshots are the same as that in Figure 1.

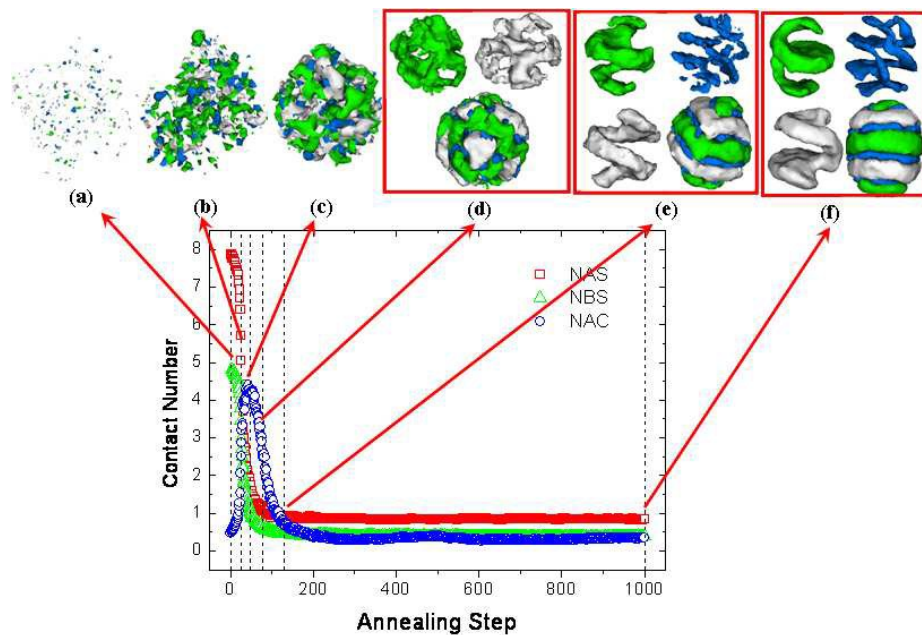
For the unique pyramid-like nanoparticle, its formation mechanism is also examined by the variations of contact numbers and a series of snapshots at different times, as shown in Figure 8. From the snapshots in Figure 8,  $A_{13}B_4C_4$  triblock copolymer firstly form a loose aggregate (Figure 8a and 8b), and then A blocks form a polyhedral core, whereas B and C blocks aggregate some small Janus lamellae on the surface of A-core, as shown in Figure 8c. As time further increases, the polyhedral A-core transitions into a tetrahedral shape, whereas small Janus B-C lamellae coalesce into four big Janus lamellae adhered onto the four surfaces of the tetrahedron, as shown in Figure 8c-8f. The variations of the contact numbers with time are also

presented in Figure 8. Similarly,  $N_{AC}$  increases to the maximum value when  $A_{13}B_4C_4$  triblock copolymers form a loose aggregate ( $t=141$ , Figure 8b), and then declines because of the microphase separation between A, B and C blocks.  $N_{AS}$  and  $N_{BS}$  show a steady decline with time during the micellization ( $t \leq 280$ ), and then remain mostly unchanged as time further increases ( $t > 280$ ). The formation mechanisms of the nanoparticle containing helical A, B and C structures and the ellipsoidal pupa-like nanoparticle are also investigated, as shown in Figure 9 and 10. Similarly, ABC triblock copolymers firstly aggregate into a loose aggregate, then the microphase separation between the immiscible A, B and C occurs, resulting in the formation of the final nanostructures.

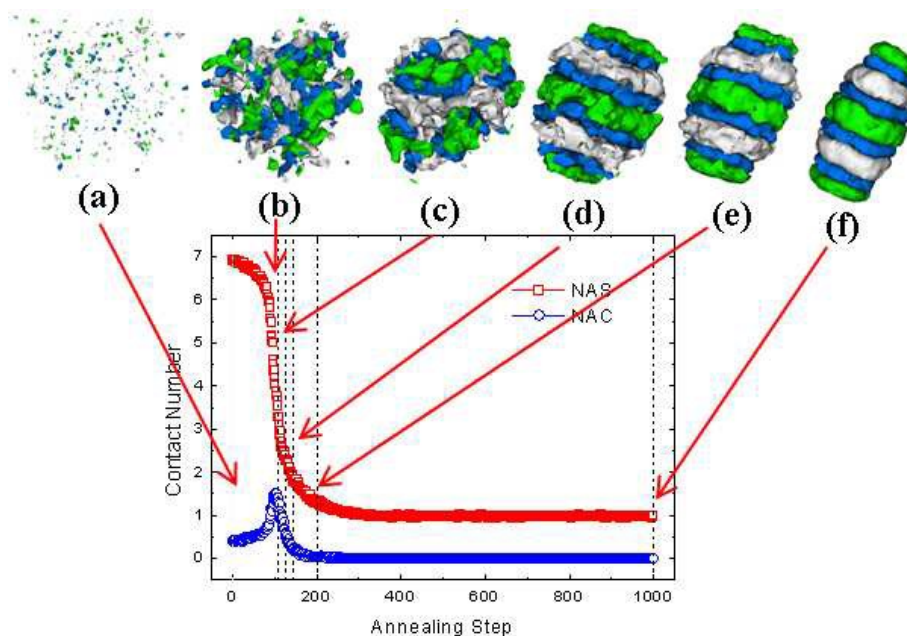


**Figure 8.** Variations of the numbers of contacts,  $N_{AS}$ ,  $N_{BS}$  and  $N_{AC}$ , with time for asymmetrical  $A_{13}B_4C_4$  triblock copolymer at  $\epsilon_{AS}=\epsilon_{BS}=\epsilon_{CS}=2.0$ . Typical snapshots at different times are also inserted in this diagram to show the formation pathway of the nanoparticle with a pyramid-like A-core and four Janus BC lamellae adhered onto the four surfaces of the pyramid-like A-core: (a)

$t=1$ ; (b)  $t=137$ ; (c)  $t=280$ ; (d)  $t=370$ ; (e)  $t=600$ ; (f)  $t=1000$ . The color codes for the snapshots are the same as that in Figure 1.



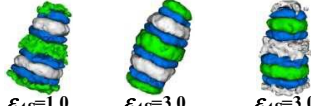
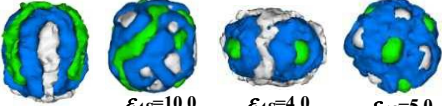
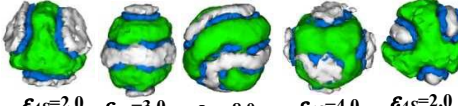
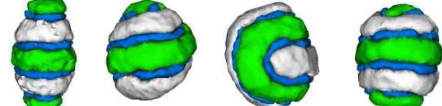
**Figure 9.** Variations of the numbers of contacts,  $N_{AS}$ ,  $N_{BS}$  and  $N_{AC}$ , with time for asymmetrical  $A_8B_5C_8$  triblock copolymer at  $\varepsilon_{AS}=\varepsilon_{BS}=\varepsilon_{CS}=9.0$ . Typical snapshots at different times are also inserted in this diagram to show the formation pathway of the nanoparticle containing helical A, B and C structures: (a)  $t=1$ ; (b)  $t=26$ ; (c)  $t=47$ ; (d)  $t=78$ ; (e)  $t=130$ ; (f)  $t=1000$ . The color codes for the snapshots are the same as that in Figure 1.



**Figure 10.** Variations of the numbers of contacts,  $N_{AS}$ ,  $N_{BS}$  and  $N_{AC}$ , with time for symmetrical  $A_7B_7C_7$  triblock copolymer at  $\varepsilon_{AS}=\varepsilon_{BS}=\varepsilon_{CS}=3.0$ . Typical snapshots at different times are also inserted in this diagram to show the formation pathway of ellipsoidal pupa-like nanoparticle: (a)  $t=1$ ; (b)  $t=107$ ; (c)  $t=125$ ; (d)  $t=142$ ; (e)  $t=200$ ; (f)  $t=1000$ . The color codes for the snapshots are the same as that in Figure 1.

To better understand the inner relationship between the self-assembled nanostructures with the block copolymer architectures, the incompatibilities between different block types, and solvent properties, we summarized all the predicted nanostructures in Table 1.

**Table 1.** Summarization of the predicted nanostructures as a function of block copolymer architectures, the incompatibilities between different block types, and solvent properties.

ABC triblock copolymer	Self-assembled nanostructures
$A_7B_7C_7$	 $\epsilon_{AS}=1.0$ $\epsilon_{AS}=3.0$ $\epsilon_{AS}=3.0$ $\epsilon_{BS}=2.0$ $\epsilon_{BS}=3.0$ $\epsilon_{BS}=2.0$ $\epsilon_{CS}=3.0$ $\epsilon_{CS}=3.0$ $\epsilon_{CS}=1.0$
$A_4B_{13}C_4$	 $\epsilon_{AS}=2.0$ $\epsilon_{AS}=10.0$ $\epsilon_{AS}=4.0$ $\epsilon_{AS}=5.0$ $\epsilon_{BS}=2.0$ $\epsilon_{BS}=10.0$ $\epsilon_{BS}=2.0$ $\epsilon_{BS}=2.0$ $\epsilon_{CS}=2.0$ $\epsilon_{CS}=10.0$ $\epsilon_{CS}=2.0$ $\epsilon_{CS}=5.0$
$A_{13}B_4C_4$	 $\epsilon_{AS}=2.0$ $\epsilon_{AS}=3.0$ $\epsilon_{AS}=8.0$ $\epsilon_{AS}=4.0$ $\epsilon_{AS}=2.0$ $\epsilon_{BS}=2.0$ $\epsilon_{BS}=3.0$ $\epsilon_{BS}=8.0$ $\epsilon_{BS}=3.0$ $\epsilon_{BS}=2.0$ $\epsilon_{CS}=2.0$ $\epsilon_{CS}=3.0$ $\epsilon_{CS}=8.0$ $\epsilon_{CS}=2.0$ $\epsilon_{CS}=4.0$
$A_8B_5C_8$	 $\epsilon_{AS}=3.0$ $\epsilon_{AS}=7.0$ $\epsilon_{AS}=8.0$ $\epsilon_{AS}=9.0$ $\epsilon_{BS}=3.0$ $\epsilon_{BS}=7.0$ $\epsilon_{BS}=8.0$ $\epsilon_{BS}=9.0$ $\epsilon_{CS}=3.0$ $\epsilon_{CS}=7.0$ $\epsilon_{CS}=8.0$ $\epsilon_{CS}=9.0$

Conclusions

Using the Monte Carlo technique, the self-assembly of ABC triblock copolymers under 3D soft-confinement is systematically investigated by varying a series of control parameters, such as the symmetry of the ABC triblock copolymer, incompatibility between the different types of the blocks, and the solvent quality for the solvophobic blocks. A rich variety of novel nanostructures are obtained via the Monte Carlo simulations. The relationship between the self-assembled nanostructures and the control parameters, such as the symmetry of the block copolymer, incompatibilities between different block types, and solvent properties, are revealed, which helps to design the novel nanostructures in experiment. Moreover, the formation pathways of some typical self-assembled nanostructures imply that the ABC triblock copolymers tend to form a loose aggregate at first, and then the



microphase separation between A, B and C blocks occurs due to the immiscibility, resulting in the formation of the unique nanostructures.

### Acknowledgements

This work was financially supported by the National Natural Science Foundation of China for General Program (51373172), Major Program (51433009), and the Open Project of State Key Laboratory of Supramolecular Structure and Materials (sklssm2015030).

### References

1. X. H. He, M. Song, H. J. Liang and C. Y. Pan, *J. Chem. Phys.*, 2001, **114**, 10510-10513.
2. A. C. Arsenault, D. A. Rider, N. Tetreault, J. I. L. Chen, N. Coombs, G. A. Ozin and I. Manners, *J. Am. Chem. Soc.*, 2005, **127**, 9954-9955.
3. B. Yu, B. Li, Q. Jin, D. Ding and A.-C. Shi, *Macromolecules*, 2007, **40**, 9133-9142.
4. Y. Zhu and W. Jiang, *Macromolecules*, 2007, **40**, 2872-2881.
5. P. Chen, H. Liang and A.-C. Shi, *Macromolecules*, 2008, **41**, 8938-8943.
6. T. Tanaka, N. Saito and M. Okubo, *Macromolecules*, 2009, **42**, 7423-7429.
7. P. Chi, Z. Wang, B. Li and A.-C. Shi, *Langmuir*, 2011, **27**, 11683-11689.
8. N. Yan, Y. Sheng, H. Liu, Y. Zhu and W. Jiang, *Langmuir*, 2015, **31**, 1660-1669.
9. H. H. Pham, I. Gourevich, J. K. Oh, J. E. N. Jonkman and E. Kumacheva, *Adv. Mater.*, 2004, **16**, 516-520.
10. J. Y. Cheng, C. A. Ross, H. I. Smith and E. L. Thomas, *Adv. Mater.*, 2006, **18**, 2505-2521.
11. R. Deng, F. Liang, X. Qu, Q. Wang, J. Zhu and Z. Yang, *Macromolecules*, 2015, **48**, 750-755.
12. D. Klinger, C. X. Wang, L. A. Connal, D. J. Audus, S. G. Jang, S. Kraemer, K. L. Killops, G. H. Fredrickson, E. J. Kramer and C. J. Hawker, *Angew. Chem., Int. Ed.*, 2014, **53**, 7018-7022.
13. S.-J. Jeon, G.-R. Yi and S.-M. Yang, *Adv. Mater.*, 2008, **20**, 4103-4108.
14. R. Deng, S. Liu, J. Li, Y. Liao, J. Tao and J. Zhu, *Adv. Mater.*, 2012, **24**, 1889-1893.
15. R. Deng, F. Liang, W. Li, S. Liu, R. Liang, M. Cai, Z. Yang and J. Zhu, *Small*, 2013, **9**, 4099-4103.
16. J. Zhu and R. C. Hayward, *Macromolecules*, 2008, **41**, 7794-7797.
17. J. Xu, K. Wang, J. Li, H. Zhou, X. Xie and J. Zhu, *Macromolecules*, 2015, **48**, 2628-2636.
18. Y. Sheng, J. An and Y. Zhu, *Chem. Phys.*, 2015, **452**, 46-52.
19. B. Yu, J. Deng, B. Li and A.-C. Shi, *Soft Matter*, 2014, **10**, 6831-6843.
20. D. J. Pochan, Z. Y. Chen, H. G. Cui, K. Hales, K. Qi and K. L. Wooley, *Science*, 2004, **306**, 94-97.

21. J. T. Zhu and W. Jiang, *Macromolecules*, 2005, **38**, 9315-9323.
22. H. Cui, Z. Chen, S. Zhong, K. L. Wooley and D. J. Pochan, *Science*, 2007, **317**, 647-650.
23. S. Zhong, H. Cui, Z. Chen, K. L. Wooley and D. J. Pochan, *Soft Matter*, 2008, **4**, 90-93.
24. J. Dupont, G. Liu, K.-i. Niihara, R. Kimoto and H. Jinnai, *Angew. Chem., Int. Ed.*, 2009, **48**, 6144-6147.
25. W. Kong, B. Li, Q. Jin, D. Ding and A.-C. Shi, *J. Am. Chem. Soc.*, 2009, **131**, 8503-8512.
26. J. Dupont and G. Liu, *Soft Matter*, 2010, **6**, 3654-3661.
27. Y. Zhu, X. Yang, W. Kong, Y. Sheng and N. Yan, *Soft Matter*, 2012, **8**, 11156-11162.
28. Y. Zhu, H. Yu, Y. Wang, J. Cui, W. Kong and W. Jiang, *Soft Matter*, 2012, **8**, 4695-4707.
29. W. Kong, W. Jiang, Y. Zhu and B. Li, *Langmuir*, 2012, **28**, 11714-11724.
30. Y. Sheng, N. Yan, J. An and Y. Zhu, *Chem. Phys.*, 2014, **441**, 47-52.
31. Z. Li, M. A. Hillmyer and T. P. Lodge, *Langmuir*, 2006, **22**, 9409-9417.
32. S. Li, Y. Jiang and J. Z. Y. Chen, *Soft Matter*, 2013, **9**, 4843-4854.
33. R. G. Larson, L. E. Scriven and H. T. Davis, *J. Chem. Phys.*, 1985, **83**, 2411-2420.
34. R. G. Larson, *J. Chem. Phys.*, 1988, **89**, 1642-1650.
35. R. G. Larson, *J. Chem. Phys.*, 1989, **91**, 2479-2488.
36. K. R. Haire, T. J. Carver and A. H. Windle, *Comput. Theor. Polym. Sci.*, 2001, **11**, 17-28.
37. S. C. Ji and J. D. Ding, *Langmuir*, 2006, **22**, 553-559.
38. N. Metropolis, A. W. Rosenbluth, M. N. Rosenbluth, A. H. Teller and E. Teller, *J. Chem. Phys.*, 1953, **21**, 1087-1092.
39. R. Deng, F. Liang, W. Li, Z. Yang and J. Zhu, *Macromolecules*, 2013, **46**, 7012-7017.
40. Y. Han, H. Yu, H. Du and W. Jiang, *J. Am. Chem. Soc.*, 2010, **132**, 1144-1150.
41. Y. Sheng, X. Yang, N. Yan and Y. Zhu, *Soft Matter*, 2013, **9**, 6254-6262.
42. J. Cui and W. Jiang, *Langmuir*, 2010, **26**, 13672-13676.

**A table of contents entry**



# Self-Assembly of ABC Triblock Copolymer under 3D Soft Confinement: A Monte

## Carlo Study

Nan Yan, Yutian Zhu, Wei Jiang

A series of novel morphologies obtained by self-assembly of ABC triblock copolymers under 3D soft confinement.

